Calorimetric Studies of the Gel–Fluid (L_β–L_α) and Lamellar–Inverted Hexagonal (L_α–H_{II}) Phase Transitions in Dialkyl- and Diacylphosphatidylethanolamines†

John M. Seddon,* Gregor Cevc,‡ and Derek Marsh

ABSTRACT: The lamellar gel-to-fluid and lamellar-to-inverted hexagonal phase transitions have been studied for a series of dialkyl- and diacylphosphatidylethanolamines and their analogues in aqueous dispersion, using differential scanning calorimetry. The phases were identified by X-ray diffraction. The enthalpy and entropy of the gel–fluid transition increase linearly with chain length with increments per chain ΔH_{inc} = 2.13 (2.34) kJ·mol^{-1}·CH$_2^{-1}$ and ΔS_{inc} = 5.61 (6.07) J·mol^{-1}·K^{-1}·CH$_2^{-1}$, respectively, for dialkylphosphatidylethanolamines (diacylphosphatidylethanolamines) over the range C12–C18 (C12–C20). The enthalpies and entropies of the lamellar–hexagonal transition are much smaller, ΔH_h = 6.1 (1.3) kJ·mol^{-1} and ΔS_h = 16.9 (3.1) J·mol^{-1}·K^{-1} for dihexadecylphosphatidylethanolamine (dipalmitoylphosphatidylethanolamine), and increase approximately linearly with chain length, ΔH_{inc} = 0.71 (0.25) kJ·mol^{-1}·CH$_2^{-1}$ and ΔS_{inc} = 1.97 (0.71) J·mol^{-1}·K^{-1}·CH$_2^{-1}$ for dialkylphosphatidylethanolamines (diacylphosphatidylethanolamines). The transition temperatures increase with increasing chain length, n, for the gel–fluid transition but decrease for the hexagonal transition according to a $1/(n - n_0')$ dependence, where n_0' is the extrapolated value at which ΔS becomes zero. Increasing salt concentration increases the gel-to-fluid transition and decreases the hexagonal transition temperatures by $\Delta T_t \approx 1.2$ (0.9) °C/mol of NaCl and $\Delta T_h \approx 3.5$ (7.3) °C/mol of NaCl for ditetradecylphosphatidylethanolamine (dimyristoylphosphatidylethanolamine), respectively. Increasing hydration decreases the gel-to-fluid transition temperature of didodecylphosphatidylethanolamine from 65 °C at 1 H$_2$O/lipid to 35 °C at a limiting hydration of 6 H$_2$O/lipid and increases the lamellar–hexagonal transition from 65 °C at 1 H$_2$O/lipid to 110 °C at a limiting hydration of 9 H$_2$O/lipid. pH titration of didodecylphosphatidylethanolamine in 2.4 M NaCl decreases the hexagonal transition by 41 °C and increases the gel-to-fluid transition by 6 °C on protonation of the phosphate group ($pK_1^i \approx 1.7$). On deprotonation of the amine group ($pK_2^i \approx 9.8$) the gel-to-fluid transition temperature decreases by 35 °C, and the hexagonal transition temperature increases by 50 °C on partial deprotonation at pH 9.3. Stepwise increase of the phosphate–amine distance from ditetradecylphosphatidylethanolamine to phosphatidylpentanolamine and increase of the degree of N-methylation from phosphatidylethanolamine to phosphatidylcholine produce a progressive decrease in temperature of the gel-to-fluid transition and, at least initially, a progressive increase of the hexagonal transition temperature. The opposite effects of these structural modifications and ionic perturbations on the two thermotropic phase transitions reflect the inverted nature of the hexagonal phase.

Although a wide range of phospholipids spontaneously form bilayers when dispersed in water, nonlamellar structures such as the inverted hexagonal (H_{II}) phase are also found under certain conditions [see, e.g., Luzzati (1968); Cullis & de Kruijff, 1979; Marsh, 1982; Seddon, 1980]. These nonbilayer phases may well be involved in activated membrane processes such as membrane fusion, synthesis, or biogenesis in which the normal lamellar membrane topology is interrupted. Studies of bilayer-to-nonlamellar phase transformations can give detailed information about the nonbilayer phase, and the phase transition itself is of particular interest since it may be involved in the mechanism of the activated membrane processes. This latter point is of special relevance, since these phase transformations are of extremely low entropy and thus can be triggered by energetically very weak interactions.

We have taken the bilayer-to-inverted hexagonal phase transition as a model for nonlamellar transformations in membranes. Hexagonal transitions in disaturated phosphatidylethanolamines have previously been reported by Harlos & Eibl (1980, 1981) and Boggs et al. (1981). In the present work systematic calorimetric measurements of the L_α–H_{II} transitions of disaturated alkyl- and acylphosphatidylethanolamines have been made as a function of hydration, pH, and salt concentration. In addition we have investigated the phospholipid chain length dependence of the transition and the effect of varying the head-group structure. Comparison with corresponding data for the lamellar gel-to-fluid transition reveals exactly opposite effects, reflecting the inverted nature of the H_{II} phase. A detailed picture emerges of the molecular and ionic factors influencing the stability of the inverted hexagonal phase.

Materials and Methods

Chemicals. Ester-linked phosphatidylethanolamines DLPE,[1] DMPE, DPPE, DSPE, puriss grade, and DAPE, purum grade, were obtained from Fluka, Buchs, Switzerland. DHPE, re-

† From the Max-Planck-Institut für biophysikalische Chemie, Abteilung Spektroskopie, D-3400 Göttingen, Federal Republic of Germany. *Received August 20, 1982.* J.M.S. was in receipt of a long-term EMBO fellowship.

‡ Permanent address: Institute for Biophysics and Institute Josef Stefan, University E. Kardelj, 6100 Ljubljana, Yugoslavia.

[1] Abbreviations: DLPE, DMPE, DPPE, DSPE, and DAPE, 1,2-dilauroyl-, 1,2-dimyristoyl-, 1,2-dipalmitoyl-, 1,2-distearoyl-, and 1,2-diarachinoyl-*sn*-glycero-3-phosphoethanolamine; DDPE, DTPE, and DOPE, 1,2-didodecyl-, 1,2-ditetradecyl-, and 1,2-dioctadecyl-*rac*-glycero-3-phosphoethanolamine; DHPE, 1,2-dihexadecyl-*sn*-glycero-3-phosphoethanolamine; DTPPent, DTPP, and DTPB, 1,2-ditetradecyl-*rac*-glycero-3-phosphopentanolamine, -phosphopropanolamine, and -phosphobutanolamine; DT(1M)PE and DT(2M)PE, 1,2-ditetradecyl-*rac*-glycero-3-phospho-*N*-methylethanolamine and -*N*,*N*-dimethylethanolamine; DTPC, 1,2-ditetradecyl-*rac*-glycero-3-phosphocholine; EDTA, ethylenediaminetetraacetic acid; DSC, differential scanning calorimetry; NMR, nuclear magnetic resonance; TLC, thin-layer chromatography; J, ionic strength.

0006-2960/83/0422-1280$01.50/0

search grade, was from Serva, Heidelberg, West Germany. Other ether-linked phosphatidylethanolamines DDPE, DTPE, and DOPE were synthesized as described below, as were the phosphatidylethanolamine analogues with different head-group structures. The purity of all synthesized and purchased phospholipids was checked both before and after measurement, by TLC in a solvent system of $CHCl_3/CH_3OH/33\%$ NH_3 (65/35/5), and staining with ninhydrin and molybdenum blue, followed by sulfuric acid charring. NaCl from Merck, Darmstadt, West Germany, was of "suprapur" grade. Buffers contained 10 μM EDTA and were prepared from analar grade chemicals.

Lipid Synthesis. 1,2-Dialkyl-*rac*-glycero-3-phosphoalkanolamines were made from the *rac*-glycerol 1,2-dialkyl ethers essentially according to the synthetic route of Eibl (1978). The length of the head-group segment, *x*-*N*-aminoalkyl ester of phosphoric acid, was $x = 2$–5 for the phosphoethanolamine through to the phosphopentanolamine, respectively. Synthesis of *rac*-glycerol 1,2-didodecyl ether, *rac*-glycerol 1,2-ditetradecyl ether, *rac*-glycerol 1,2-dihexadecyl ether, and *rac*-glycerol 1,2-dioctadecyl ether will be described in detail elsewhere. The appropriate glycerol dialkyl ether (0.01 mol) in 10 mL of tetrahydrofuran was stirred and cooled on ice. After the addition of triethylamine (0.015 mol) and phosphorus oxychloride (each in 5 mL of tetrahydrofuran), the reaction mixture was kept at 0 °C for 15 min and subsequently at 20 °C until TLC on silicic acid plates ($CHCl_3/CH_3OH/33\%$ NH_3, 200/15/1) showed that most of the starting material was converted into the 1,2-dialkyl-*rac*-glycero-3-phosphoric acid dichloride. The precipitated triethylamine hydrochloride was removed by suction filtering in the absence of moisture. After the first drying the mixture was rotary evaporated for a second time, from toluene. Then, another 30 mL of tetrahydrofuran containing 0.015 mol of triethylamine was added to the reaction vessel, followed by the appropriate amino alcohol, all at 15 °C. The formation of the intermediate oxazophospholane was followed by TLC, and after no further changes were seen, the temperature of the mixture was increased to 40 °C for a further 60 min. The mixture was then brought to dryness by rotary evaporation and redissolved in 2-propanol. Addition of 10% formic acid caused hydrolysis of the oxazophospholane and precipitation of the corresponding phosphoalkanolamine. After 3 h, the latter was extracted with $CHCl_3/CH_3OH$, shaken against 0.5 M Na_2CO_3, and condensed on a rotary evaporator. After the mixture was redissolved in a small volume of $CHCl_3$, the raw product was finally precipitated on ice from acetone. The total yields based on the glycerol dialkyl ethers were 90% and >60%, the latter value corresponding to the longest amino alcohol used.

The crude products were purified by column chromatography by using Kieselgel 60 (Merck, Darmstadt, West Germany). $CHCl_3/CH_3OH/33\%$ NH_3 mixtures were used for elution, starting with 200/15/1 (v/v) and increasing the polarity of the solvent stepwise up to 65/30/3. The purified dialkylglycerophosphoalkanolamines were then finally crystallized from acetone on ice, dried in vacuo (<15 Pa), and stored at −20 °C until needed for experiments. Anal. Calcd for DDPE: C, 63.12; H, 11.33; O, 17.40; N, 2.54; P, 5.61. Found: C, 62.97; H, 11.23; O, 17.61; N, 2.50; P, 5.69. Anal. Calcd for DTPE: C, 65.20; H, 11.61; O, 15.75; N, 2.30; P, 5.10. Found: C, 65.20; H, 11.58; O, 15.71; N, 2.32; P, 5.19. Anal. Calcd for DOPE: C, 67.46; H, 12.04; O, 13.33; N, 1.95; P, 4.30. Found: C, 67.48; H, 12.10; O, 14.07; N, 1.89; P, 4.46. Anal. Calcd for DTPP·$2H_2O$: C, 62.07; H, 11.64; O, 19.45; N, 2.13; P, 4.70. Found: C, 60.98; H, 11.35; O, 18.75; N, 2.66; P, 6.26. Anal. Calcd for DTPB: C, 66.10; H, 11.73; O, 15.10; N, 2.20; P, 4.87. Found: C, 66.29; H, 11.68; O, 14.81; N, 2.28; P, 4.94.

The N-methylated 1,2-dialkyl-*rac*-glycero-3-phosphoethanolamines were produced by different methods depending on the degree of methylation. 1,2-Ditetradecyl-*rac*-glycero-3-phospho-*N*-methylethanolamine was prepared essentially according to the procedure described above for DTPE, except that *N*-methylethanolamine (Fluka, Buchs, Switzerland, practical grade) was used instead of 2-aminoethanol. 1,2-Ditetradecyl-*rac*-glycero-3-phospho-*N*,*N*-dimethylethanolamine was prepared by using 2-bromoethanol (Eibl & Nicksch, 1978) to produce the intermediate phosphatidic acid bromoethyl ester which was then aminated with dimethylamine (0.0125 mol, Fluka, purum) to yield >85% of the desired phospho-*N*,*N*-dimethylethanolamine. 1,2-Ditetradecyl-*rac*-glycero-3-phosphocholine was prepared by complete N-methylation of DTPE using CH_3I in $CHCl_3/CH_3OH$. The synthesis followed Stockton et al. (1974), except that the reaction was stopped after 72 h, since TLC indicated that the reaction was then >80% completed. The lipid purification was as described above. Anal. Calcd for DT(1M)PE·H_2O: C, 63.80; H, 11.66; O, 17.50; N, 2.19; P, 4.84. Found: C, 64.43; H, 11.87; O, 16.73; N, 2.21; P, 4.76. Anal. Calcd for DT-(2M)PE·H_2O: C, 64.62; H, 11.71; O, 17.12; N, 2.14; P, 4.74. Found: C, 64.23; H, 11.98; O, 16.43; N, 2.37; P, 4.60. Anal. Calcd for DTPC·$2H_2O$: C, 63.03; H, 11.75; O, 18.66; N, 2.04; P, 4.51. Found: C, 62.44; H, 11.75; O, 18.83; N, 2.00; P, 4.98.

Calorimetry. Measurements were made on a Perkin-Elmer "DSC 2" differential scanning calorimeter fitted with an "Intracooler 1". Dry phospholipid (5–10 mg) was weighed into "large-volume" stainless steel pans, 40 μL of water or buffer was then added, and the pans were sealed. The reference pan contained 40 μL of buffer. The heating rate was 2.5 °C/min, except where otherwise stated. The transition temperatures and enthalpies were calibrated with indium and octadecane. The transition temperature was taken as the intercept of the tangent of the rising slope with the base line (estimated accuracy ±0.5 °C, gel–fluid transition; ±1 °C, hexagonal transition). The enthalpies were determined by paper weighing; three to six samples were measured for each lipid (estimated accuracy ±5%, gel–fluid transition; ±15%, hexagonal transition). Additional transitions were normally observed on the first heating scan due to incomplete initial hydration of the lipid. The samples were scanned repeatedly until reproducible transition temperatures were obtained. Only the heating scans were analyzed.

For the hydration studies, the lipids were dried under vacuum over P_2O_5 for 3 days. The accuracy of the water content, as determined from the weight of the sealed pans, was estimated to be +1.5 or −0.5 H_2O/lipid. (The additional +1.0 error limit comes from the uncertainty in achieving complete dehydration.) Optimal hydration was ensured by scanning the sample up to 100 °C between 4 and 8 times. For the pH titration, the following buffers were employed: NaCl/HCl, Na_2HPO_4/KH_2PO_4, $(HOCH_2CH_2)_3N$, $Na_2B_4O_7$/NaOH, and NaCl/NaOH. The ionic strengths of these buffers were $0.05 \leq J \leq 0.1$ M. A 5-mg sample of dry lipid was dispersed in excess (400 μL) buffer, and the lipid pellet for DSC measurement was obtained by centrifugation. Sample pH was determined from the supernatants (accuracy ±0.1 pH unit).

X-ray Diffraction. A Guinier camera fitted with a bent quartz crystal monochromator was used (R. Huber, 8211 Reinsting, West Germany). The monochromator was adjusted

Table I: Phase Transition Temperatures (°C), Enthalpies [kJ mol^{-1} (kcal mol^{-1})], and Entropies [J mol^{-1} K^{-1} (cal mol^{-1} K^{-1})] of Dialkyl- and Diacylphosphatidylethanolamines in H_2O[a]

	gel-fluid			bilayer-hexagonal		
chain length	T_t	ΔH	ΔS	T_h	ΔH	ΔS
dialkyl						
12	35	16.1 (3.8)	52 (12.5)	110	0.4 (0.1)	1.1 (0.3)
14	55.5	24.0 (5.7)	73 (17.5)	96	3.0 (0.7)	8.2 (2.0)
16	68.5	33.1 (7.9)	97 (23.2)	86	6.1 (1.5)	16.9 (4.0)
18	77	39.1 (9.4)	112 (26.7)	81	6.9 (1.7)	19.5 (4.7)
increment per CH_2		2.13 (0.51)	5.61 (1.34)		0.71 (0.17)	1.97 (0.47)
intercept		−35.4 (−8.5)	−83.0 (−19.8)		−16.6 (−3.2)	−46.7 (−11.2)
diacyl						
12	30.5	15.7 (3.7)	51.5 (12.3)			
14	49.5	24.2 (5.8)	75 (17.9)			
16	64	33.1 (7.9)	98 (23.5)	123	1.3 (0.3)	3.1 (0.8)
18	74	43.9 (10.5)	126 (30.2)	101	3.8 (0.9)	10.1 (2.4)
20	82.5	52.4 (12.5)	147 (35.2)	96	3.2 (0.8)	8.7 (2.1)
increment per CH_2		2.34 (0.56)	6.07 (1.45)		0.25 (0.06)	0.71 (0.17)
intercept		−40.7 (−9.7)	−94.5 (−22.6)		−6.1 (−1.5)	−17.9 (−4.3)

[a] Heating rate 2.5 K min^{-1}.

to isolate the Cu Kα_1 (λ = 0.15405 nm) radiation. The X-ray tube (AEG type F 50/21) was operated at 50 kV and 20 mA. Exposure times were typically 10 min to 2 h. The hydrated lipid samples were sealed between thin mica sheets in custom-built metal holders; the temperature was controlled to 0.5 °C by electrical heating. The X-ray film (type CEA REFLEX 15) was purchased from CEA (Caeverken AB, Strägnäs, Sweden). So that continuous temperature scans could be recorded, the sample was heated at a rate of 0.1 °C/min while the film holder was moved downward at a rate of 0.06 mm/min. The film slit width was reduced to 1 mm for these exposures.

NMR Measurements. Proton dipolar decoupled, 109-MHz ^{31}P NMR spectra were obtained with a Bruker WH-270 spectrometer, equipped with a nitrogen gas-flow temperature regulation system. The radio frequency pulse width was 10 μs. Normal free induction decays were collected with a dwell time of 16 μs, and with minimal initial delay. The decoupling power was 5–10 W, and the duty cycle of the gated decoupling was ca. 0.2%. Typically 200 mg of DDPE was mixed with the required amount of water and sealed in the bottom of a standard 10-mm NMR tube with a special Teflon/"O"-ring stopper designed to minimize evaporation loss. Samples were hydrated by preheating to 85 °C for 10–15 min. Further details of the NMR measurements can be found in Marsh & Seddon (1982).

Results

DSC scans of the homologous series of ester and ether phosphatidylethanolamines dispersed in water are shown in Figure 1: (a) C12–C20 esters; (b) C12–C18 ethers. The high-enthalpy peaks correspond to the chain-melting transition L_β–L_α. The smaller peaks at higher temperatures were found by X-ray diffraction to correspond to transitions to the hexagonal phase, H_{II}, in each case. This is in agreement with previous results obtained for DHPE in low salt (Harlos & Eibl, 1980; Boggs et al., 1981). Positive identification of the H_{II} phase of DPPE in low salt resolves previous uncertainties in this assignment (Harlos & Eibl, 1981; K. Harlos, private communication). For DHPE and DSPE supplementary identification of the hexagonal phases has also been provided by ^{31}P NMR spectroscopy (Marsh & Seddon, 1982). For DDPE the hexagonal transition may involve intermediate states, since the DSC peak is rather broad and extra diffraction lines were observed in the region of the transition. Transitions to the hexagonal phase were not detected for DLPE or DMPE

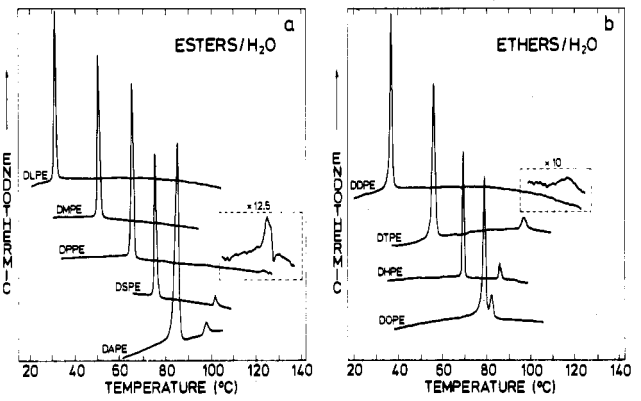

FIGURE 1: DSC traces of disaturated phosphatidylethanolamines dispersed in excess unbuffered water (ca. 8 mg/50 μL). (a) Diacyl-PEs. (b) Dialkyl-PEs. Scanning rate = 2.5 °C/min.

at temperatures up to 150 °C. Extrapolation of the results in Figure 1a suggests that the hexagonal transition, if it exists for these lipids, should lie above 150 °C. The minor transition observed at 43 °C in DLPE by Wilkinson & Nagle (1981), and suggested to correspond to a hexagonal transition, actually corresponds to the chain melting of a crystalline form of the lipid in excess water (Seddon et al., 1983).

A representative temperature scan of the diffraction pattern of DHPE in excess water is shown in Figure 2. This clearly indicates both the transitions observed by calorimetry. At 68 °C the gel–fluid lamellar transition is accompanied by the disappearance (due to broadening) of the sharp chain–chain diffraction line in the wide-angle region, and by an abrupt increase in the lamellar spacing observed at low angle. At 87–91 °C there is a discontinuous change in the low-angle region yielding long spacings in the ratio $1:1/3^{1/2}:1/2$ . . . characteristic of a hexagonal arrangement of lipid cylinders.

The calorimetric results for both ester and ether PEs in water are summarized in Table I. Values for the main transition of DAPE, DDPE, and DOPE are reported for the first time; the remaining values for the main transition are in agreement with the results of previous workers [see Seelig (1981), Harlos & Eibl (1981), and Boggs et al. (1981)]. Values for the hexagonal transition in low salt have been previously reported only for DHPE and DSPE (Harlos & Eibl, 1981; Boggs et al., 1981) and are in agreement with the present results. [Hexagonal transitions have also been previously detected by Harlos & Eibl (1981) in DTPE and DPPE at high salt.]

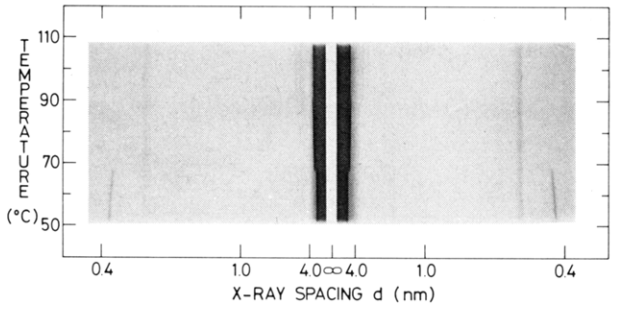

FIGURE 2: Continuous temperature scan of the X-ray diffraction pattern of DHPE dispersion in unbuffered water. The X-ray film was scanned down behind a masking slit, while the sample was continuously heated. Heating rate = 0.1 °C/min. The broad line at 0.5 nm arises from the sample holder.

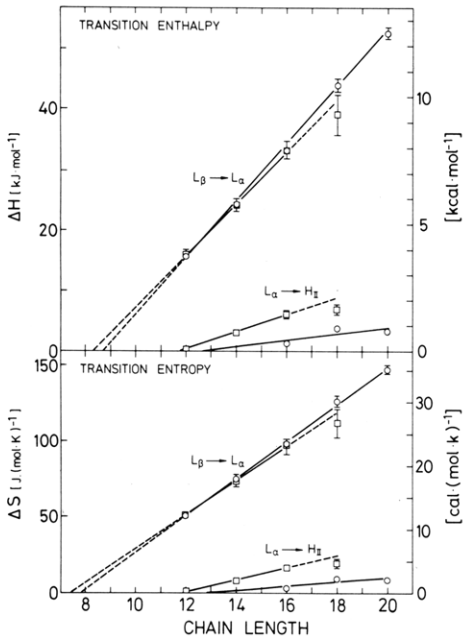

FIGURE 3: Chain length dependence of the transition enthalpy (upper) and transition entropy (lower) of the gel-to-fluid ($L_\beta \rightarrow L_\alpha$) and lamellar-to-inverted hexagonal ($L_\alpha \rightarrow H_{II}$) phase transitions of dialkyl (□) and diacyl (○) phosphatidylethanolamine unbuffered aqueous dispersions.

Chain Length Dependence. The dependence of the transition enthalpy, ΔH_t, and transition entropy, ΔS_t, on the lipid hydrocarbon chain length, n, is given for both ester and ether lipids in Figure 3. An approximately linear dependence of both ΔH_t and ΔS_t on chain length is found for the main transition of both ester and ether lipids. For the hexagonal transition of the ether lipids the dependence is also approximately linear. For ester lipids the situation is less clear. The results of a linear regression analysis of the data of Figure 3 are given in Table I. The chain length dependences are fitted to the expression $\Delta H_t = 2n \cdot \Delta H_{inc} + \Delta H_0$ and $\Delta S_t = 2n \cdot \Delta S_{inc} + \Delta S_0$, where ΔH_{inc} and ΔS_{inc} are the incremental transition enthalpy and entropy per CH_2 group per chain and ΔH_0 and ΔS_0 are the enthalpy and entropy intercepts extrapolated to zero chain length. The data for DOPE are anomalously low and have not been included in the linear regression.

The chain length dependence of the gel–fluid and lamellar–hexagonal transition temperatures (T_t and T_h, respectively) of ester and ether lipids at various salt concentrations is given in Figure 4. In each case the hexagonal transition temperature decreases with increasing chain length, whereas the main transition temperature increases. The hexagonal transition temperature is consistently lower for the dialkyl-PEs than for

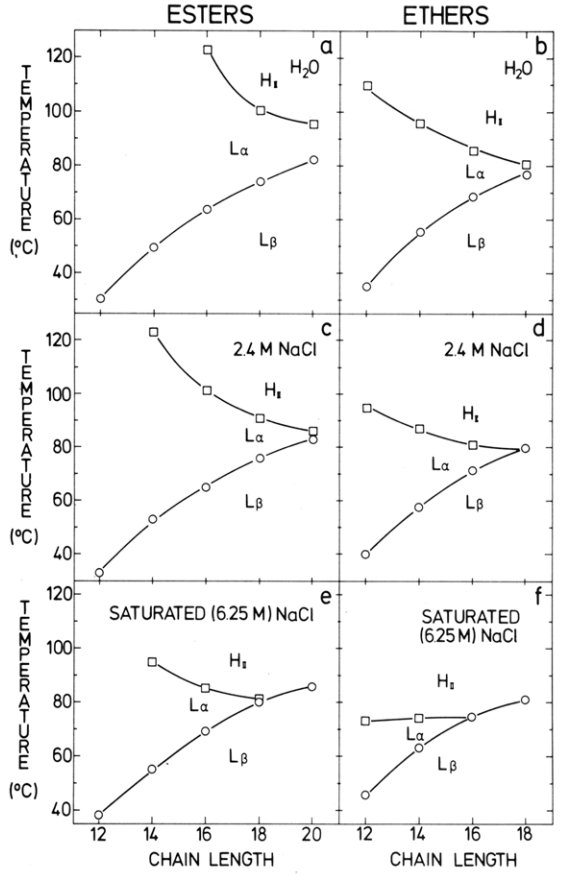

FIGURE 4: Hydrocarbon chain length dependence of the gel-to-fluid ($L_\beta \rightarrow L_\alpha$) (○) and lamellar-to-inverted hexagonal ($L_\alpha \rightarrow H_{II}$) (□) transition temperatures for (a, c, e) diacyl- and (b, d, f) dialkylphosphatidylethanolamines. (a, b) Dispersed in unbuffered water, (c, d) in 2.4 M NaCl (pH ~7), and (e, f) in saturated NaCl (pH ~7).

the diacyl lipids of the same chain length, whereas the reverse is true for the main transition. The difference between diacyl and dialkyl lipids is greater for the hexagonal transition than for the main transition. These trends are consistent with the previous, less extensive data of Harlos & Eibl (1981) and Boggs et al. (1981).

Salt Dependence. The dependence of main and hexagonal transition temperatures on bulk NaCl concentration, for diacyl and dialkyl lipids of 14 C atom chain length, is given in Figure 5. An approximately linear dependence is observed over the range studied, although there are indications of deviations from linearity, particularly for the main transition of DMPE. The effect of increasing salt concentration is in every case to increase the main transition temperature and to decrease the hexagonal transition temperature. The shifts of the hexagonal transition are always much greater than those of the main transition, as seen previously by Harlos & Eibl (1981). Comparison with Figure 4 shows similar effects for other chain lengths and also shows that the size of the salt-induced shifts increases with decreasing chain length. Figure 5 also demonstrates why a lamellar–hexagonal transition was not observed in DMPE in pure water (Figure 1); extrapolation to zero salt concentration indicates that the hexagonal transition would occur at greater than 140 °C. Increasing salt concentration is also found to sharpen and increase the enthalpy of the hexagonal transition, while the main transition is little affected in this respect. Similar results on the salt dependence of DSPE have been reported by Harlos & Eibl (1981). The fact that the results for DHPE, which is in the *sn*-2 configuration, are consistent with those for all the other dialkyl lipids, which are

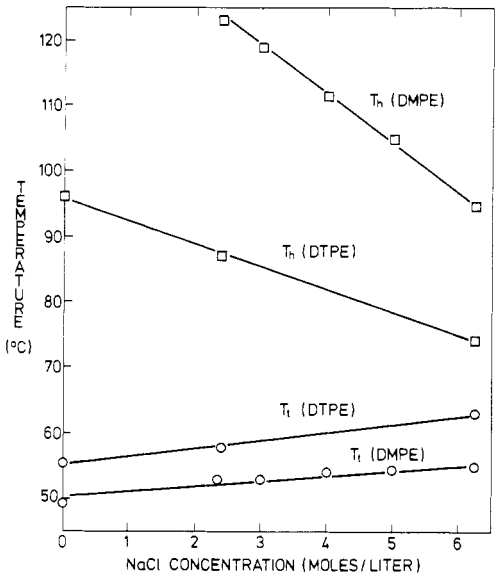

FIGURE 5: Dependence of the lamellar–hexagonal (T_h) (□) and gel–fluid (T_t) (○) phase transition temperatures on NaCl concentration for aqueous dispersions (pH ~7) of dimyristoylphosphatidylethanolamine (DMPE) and ditetradecylphosphatidylethanolamine (DTPE).

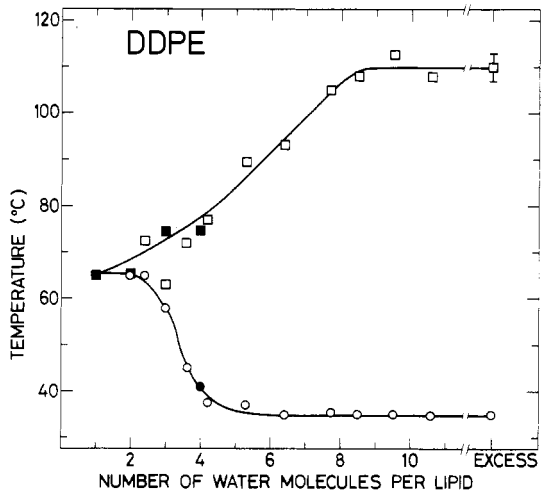

FIGURE 6: Dependence on water content (unbuffered) of the gel–fluid (○) and lamellar–hexagonal (□) phase transition temperatures of didodecylphosphatidylethanolamine. Points (●, ■) obtained by ^{31}P NMR; all others from calorimetry.

racemic mixtures, strongly suggests that the stereoisomeric configuration does not affect the thermodynamics of either the hexagonal or the gel–fluid transition.

Hydration Dependence. The dependence of the transition temperatures of DDPE on the water content of the samples is given in Figure 6. Decreasing water content increases the main transition temperature and decreases the hexagonal transition temperature. The main transition temperature first begins to rise when the water content falls below 6 water molecules/lipid. For the hexagonal transition the limiting water content determined in this way is 9 waters/lipid, implying either a greater hydration of the hexagonal phase or an increasing hydration of the L_α phase with increasing temperature. These values constitute lower estimates for the limiting hydration, since it is possible that additional water may be structurally incorporated without appreciably affecting the thermodynamics of the phase transition. Below 4 water molecules/lipid, only the first order of the diffraction pattern was observed in the fluid phase. Thus a definite identification

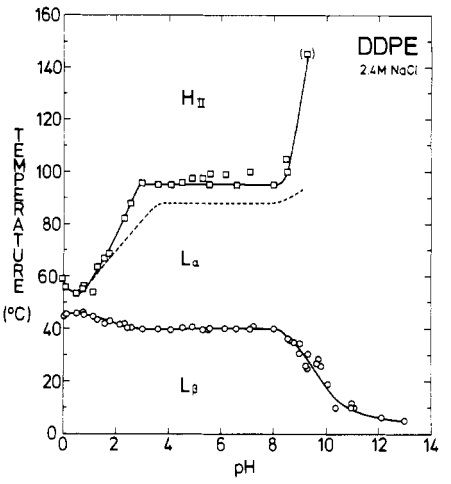

FIGURE 7: pH dependence of the gel–fluid (○) and lamellar–hexagonal (□) phase transition temperatures of didodecylphosphatidylethanolamine dispersions in 2.4 M NaCl. The dashed line indicates the appearance of additional diffraction lines in the region of the lamellar–hexagonal transition: The point in parentheses was obtained from an X-ray continuous temperature scan.

of the phases at lower water could not be made by X-ray diffraction. In this region, phase identifications were made by ^{31}P NMR (cf. Marsh & Seddon, 1982), from the characteristic halving and changing of the sign of the chemical shift anisotropy, occurring at the lamellar–hexagonal transition. Transition temperatures observed in this way by ^{31}P NMR were in good agreement with the calorimetrically determined values (see Figure 6). At, or close to, limiting hydration the fluid lamellar phase transforms directly to the hexagonal phase at T_h, with no indication of the intermediate phase of different long spacing, which was observed in excess water.

pH Titration. The variation in transition temperatures of DDPE in 2.4 M NaCl as a function of pH is given in Figure 7. The T_h value at pH 9.28 was determined only from an X-ray continuous temperature scan; all other values are from DSC. The dashed line represents the point at which the diffraction pattern of the lamellar phase starts to disappear and an intermediate unidentified phase of longer spacing appears. This phase continues for some degrees beyond the appearance of the hexagonal phase. (As seen in Figure 1, the calorimetric transition for DDPE is considerably broader than for the other lipids.) Below pH 2.3 the transition is directly from L_α to H_{II} with no trace of the intermediate phase. Certain buffers were found to perturb the transitions. Acetic and formic acid buffers depressed the main transition by ~4 °C and abolished the hexagonal calorimetric transition. The T_h values lying above the solid line at $4 < pH < 7$ were obtained with phosphate buffer. This variation of T_h is probably artifactual, since the other buffers used (see Materials and Methods) yield a constant value for T_h over this pH range. Transition temperature shifts are observed corresponding to titration of both the phosphate ($pK_1^i \approx 1.7$) and the amino group ($pK_2^i \approx 9.8$). These effective pK_as, defined by the 50% value of the main transition temperature shift, are compared with that of DMPE in low salt ($J = 0.1$) and of phosphoethanolamine in water, in Table II. The value estimated at the phosphate titration from the hexagonal transition temperature shift was slightly higher ($pK_1^i \approx 1.9$). In both cases the shift of the hexagonal transition on titration is greater than, and in the opposite sense to, that of the main transition. At the phosphate titration, the total shift of the main transition is $\Delta T_t = +6$ °C, whereas that of the hexagonal transition is $\Delta T_h = -41$ °C. Similarly, at pH 9.28, within the amine

Table II: Apparent Dissociation Constants of Phosphatidylethanolamine

compound	pK_1^i	pK_2^i	conditions	ref
DDPE	1.7	9.8	J = 2.4	this work
DMPE		11.25	J = 0.1	*a*
dimethyl hydrogen phosphate	1.22			*b*
O-phosphoryl-ethanolamine		10.13	J = 0.15	*c*
DLPE	<1	9.75	Triton X-100	*d*

[a] Cevc et al. (1981). [b] IUPAC (1979). [c] Osterberg (1962). [d] London & Feigenson (1979).

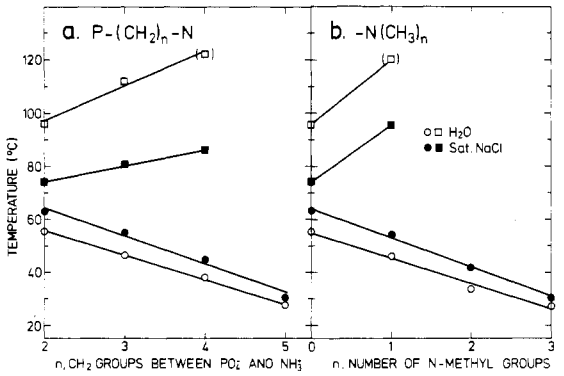

FIGURE 8: Dependence of the gel–fluid (○, ●) and lamellar–hexagonal (□, ■) phase transition temperatures on (a) the number of methylene groups separating the phosphate and amine groups and (b) the degree of N-methylation (abscissa, n = 0, PE; n = 1, monomethyl-PE; n = 2, dimethyl-PE; n = 3, phosphatidylcholine), in the polar head group of ditetradecylphosphatidylethanolamine analogues. Lipid dispersions in unbuffered water (○, □), and saturated NaCl (pH ~7) (●, ■). The points in brackets were obtained from X-ray continuous temperature scans at slightly below limiting hydration (a) and at ~10 waters/lipid (b).

titration, ΔT_t = −15 °C, whereas ΔT_h = +50 °C. The total shift of the main transition at the amine titration is ΔT_t = −35 °C, but the total titration shift of the hexagonal transition at high pH could not be observed.

Head-Group Modification. The effect of increasing the distance between the phosphate and the amine group in ditetradecylphosphatidylalkanolamines is given in Figure 8a. In saturated NaCl the gel-to-fluid transition temperature decreases linearly from 63 to 30.5 °C on increasing the number of intervening CH_2 groups from two (DTPE) to five (DTPPent), and similar results are observed in water without salt. The effect on the hexagonal transition is opposite to that on the gel-to-fluid transition. In saturated NaCl T_h increases from 74 to 86 °C on increasing the number of CH_2 groups from two (DTPE) to four (DTPB). No well-defined lamellar–hexagonal transition is observed for DTPPent [$n(CH_2)$ = 5] in saturated NaCl. X-ray diffraction results indicate that the L_α phase starts to disappear at 60 °C and additional phases of different long spacing appear; by 100 °C the hexagonal phase may also be present. In excess water without salt T_h increases from 96 to 112 °C on going from DTPE [$n(CH_2)$ = 2] to DTPP [$n(CH_2)$ = 3]. For DTPB [$n(CH_2)$ = 4] no clear hexagonal transition is observed in excess water, and X-ray diffraction indicates the presence of additional phases in the region between 80 and 138 °C, at which point the structure is predominantly hexagonal. The DTPB behavior is simpler at close to limiting hydration, remaining predominantly in the L_α phase until ~122 °C whereupon the phase becomes predominantly H_{II}. For DTPPent [$n(CH_2)$ = 5] in water only the L_α phase is observed up to 128 °C at which point a sharp transition to an unidentified nonlamellar phase of different long spacing takes place.

The effect of increasing the degree of N-methylation of the head group in DTPE analogues is given in Figure 8b. The $-NH_3^+$ methylation causes T_t to fall from 63 °C for DTPE to 30 °C for DTPC in saturated NaCl, and a similar decrease is observed in water without salt. In contrast, addition of a single methyl group causes T_h to increase from 74 (DTPE) to 96 °C [DT(1M)PE] in saturated NaCl. For DT(1M)PE in water additional phases appear between L_α and H_{II} accompanied by a broad, low-enthalpy transition at ~90 °C. The hexagonal transition, detected by X-ray diffraction, occurs at ~120 °C at ~10 waters/lipid and at ~148 °C in excess water. For the dimethyl derivative [DT(2M)PE] additional phases are observed in saturated NaCl by X-ray diffraction, but no hexagonal phase was identified. For DT(2M)PE in water and DTPC in both water and saturated NaCl, only the L_α phase is observed up to 140 °C.

Discussion

One feature which emerges from this systematic study is that the shifts of the lamellar-to-hexagonal transition, in response to those perturbations and modifications of the lipid structure that we have investigated, are in the opposite sense to the corresponding shifts of the lamellar gel-to-fluid transition. These results are consistent with previous ideas regarding the factors which influence the stability of the inverted hexagonal phase (Luzzati, 1968; Shipley, 1973). The magnitude of the shifts in response to ionic perturbations is much greater for the hexagonal than for the gel–fluid transition. This arises predominantly from the low entropy of the hexagonal transition, which causes it to be very sensitive to perturbations. The transition temperature shift due to a perturbation, G^{int}, of the bilayer free energy is given by (Träuble, 1976)

$$\Delta T_t^{int} = \Delta G_t^{int} / \Delta S_t^* \quad (1)$$

where ΔG_t^{int} is the change in G^{int} at the phase transition and ΔS_t^* is the transition entropy of the unperturbed system. For head-group perturbations, the opposite sense of the hexagonal transition shifts relative to the gel-to-fluid transition arises basically from the fact that the lamellar-to-hexagonal transition is accompanied by a decrease in area per molecule at the lipid head groups (Reiss-Husson, 1967; J. M. Seddon, G. Cevc, R. D. Kaye, and D. Marsh, unpublished results), whereas the lamellar gel-to-fluid transition is accompanied by an increase in molecular area [see, e.g., Marsh (1982)]. Thus interactions which tend to expand the area of the head groups stabilize the fluid lamellar phase relative to the gel phase ($G_t^{int} < 0$), but destabilize the hexagonal phase relative to the fluid lamellar phase ($G_t^{int} > 0$) and vice versa, reflecting the inverted nature of the H_{II} phase. The opposite effect of modifications of the lipid head-group structure arises also from the inverted nature of this phase. Modifications which decrease the volume of the polar head groups relative to the hydrocarbon region will favor the hexagonal phase and the lamellar gel phase. The opposite effects of increasing chain length on the hexagonal and gel–fluid transitions are a different case, however. Unlike the effects of the head-group interactions, they do not arise from changes in molecular area. Whereas the increase in hydrocarbon volume relative to the head groups favors the hexagonal phase, the stabilization of the gel phase arises from the increase in van der Waals interactions with increasing chain length. The individual features are considered in detail below.

Chain Length Dependence. The results of Figure 3 indicate a linear dependence of both transition enthalpy and transition entropy on chain length for the gel–fluid transition, with very

similar values for the incremental change per CH_2 (Table I) to those for phosphatidylcholines (Phillips et al., 1969). Extrapolation to zero chain length gives large negative intercepts, which may be due to a preferential ordering of the chain segments close to the polar head groups and also due to water ordering arising from head-group hydration.

The entropies and enthalpies of the hexagonal transition are much smaller than for the gel–fluid transition. This indicates that there is relatively little change in the net chain ordering on going from the fluid lamellar to the hexagonal phase. A possible reason is a partial cancellation due to counterbalancing changes at opposite ends of the molecule, arising from the inverted nature of the phase (J. M. Seddon and D. Marsh, unpublished results). In this connection it is interesting to note that both ΔS_h and ΔH_h become extremely small when the chain length is decreased to 12 C atoms (Figure 3). The considerable difference between dialkyl- and diacyl-PEs observed in the calorimetric properties of the hexagonal transition indicates a rather strong influence of the chain linkage on the stability of the hexagonal phase. The hexagonal transition enthalpies and entropies again depend approximately linearly on the hydrocarbon chain length, although the incremental changes are much smaller than for the gel–fluid transition (see Table I).

The dependences of the transition temperatures on lipid chain length (Figure 4) can be phenomenologically described in terms of the linear chain length dependences of ΔH and ΔS. The latter is written as $\Delta H_t = 2(n - n_0)\Delta H_{inc}$ and $\Delta S_t = 2(n - n_0')\Delta S_{inc}$, where n_0 ($=-\Delta H_0/2\Delta H_{inc}$), and n_0' ($=-\Delta S_0/2\Delta S_{inc}$) are the chain lengths at which ΔH_t and ΔS_t, respectively, extrapolate to zero. Then, since $T_t = \Delta H_t/\Delta S_t$ for a first-order transition, the chain length dependence of the transition temperature is given by (Marsh, 1982)

$$T_t = T_t^{\infty}[1 - (n_0 - n_0')/(n - n_0')] \quad (2)$$

where $T_t^{\infty} = \Delta H_{inc}/\Delta S_{inc}$, the transition temperature extrapolated to infinite chain length, is equal to the ratio of the incremental transition enthalpy and transition entropy. It should be noted that, since ΔH_{inc} and ΔS_{inc} are both very different from the corresponding values for crystalline hydrocarbons, T_t^{∞} should not be equal to the transition temperature of polyethylene as was previously assumed (Nagle & Wilkinson, 1978). Plots of the chain length dependence of the transition temperatures, using values of n_0 and n_0' deduced from Figure 3, are given in Figure 9 and conform reasonably well to eq 2, especially for the gel–fluid transition. Intercepts and gradients of the plots also agree well numerically with the predicted expressions.

The origin of the chain length dependence of ΔH and ΔS for the gel–fluid transition is clear. The transition is accompanied by an increase in rotational isomerization and a decrease in van der Waals interactions, both of which are directly dependent on chain length. For the hexagonal transition the position is less clear. However, a simple geometric model can be used to explain some features of the chain length dependence of the hexagonal transition. According to Israelachvili et al. (1976, 1977, 1980) the free energy per molecule of the lipid bilayer, $\mu(=G/N_A)$, may be modeled by two area-dependent terms:

$$\mu = \gamma a + (C/a)(1 + D/R) \quad (3)$$

where $\gamma \approx 50$ mN·m^{-1} is the interfacial tension and represents the hydrophobic effects and head-group hydration, a being the molecular area. The second term represents the intermolecular interactions between the head groups, F_{HD}, and between the hydrocarbon chains, F_{HC}. Because the center of gravity of the

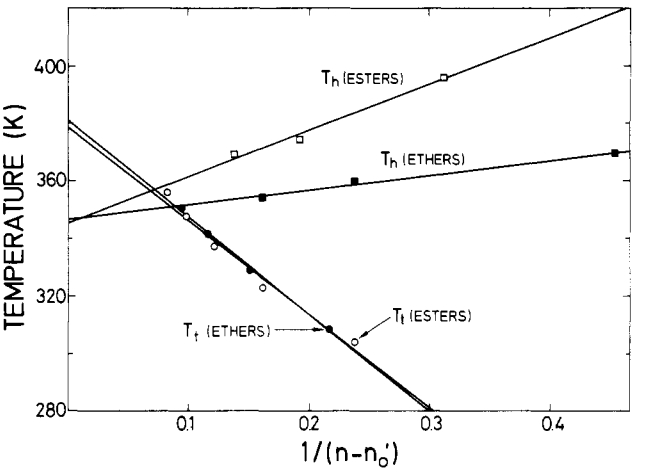

FIGURE 9: Chain length dependence of the lamellar gel-to-fluid transition temperatures, T_t (○, ●), and of the lamellar-to-inverted hexagonal transition temperatures, T_h (□, ■), for diacyl- (ester) (○, □) and dialkylphosphatidylethanolamines (ether) (●, ■). The transition temperature is plotted against $1/(n - n_0')$ where n is the number of C atoms in the chain and n_0' is the intercept in the n dependence of ΔS_t (cf. Figure 3) as explained in the text.

head-group and hydrocarbon repulsions is offset by a distance, D, from the polar–apolar interface at which the interfacial tension acts [$2D = lf - d(1 - f)$, where $f = F_{HC}/(F_{HC} + F_{HD})$ and l and d are the thickness of the hydrocarbon and polar regions, respectively], there is a spontaneous tendency to curvature, with radius of curvature, R. The free energy per molecule in the inverted hexagonal phase at equilibrium can then be shown to be

$$\mu_H = 2\gamma a_0 = 2\gamma\left(\frac{C}{1 + D/R}\right)^{1/2} \quad (4)$$

where $a_0 \approx 0.5$ nm^2 (J. M. Seddon, G. Cevc, R. D. Kaye, and D. Marsh, unpublished results) is the equilibrium area per molecule at the polar–apolar interface, R is measured from the center of the hexagonal cylinder to the polar–apolar interface, and D is measured from the polar–apolar interface into the hydrocarbon phase. Geometric changes in the hexagonal phase free energy with increasing chain length come from an increase in D: $\delta D = (f/2)[\delta l + (l + d)(1 - f)\delta F_{HC}/F_{HC}]$, where $\delta F_{HC}/F_{HC} \approx \delta l/l$. According to Israelachvili et al. (1980), $F_{HC} \sim 20$ mN·m^{-1} and $F_{HP} \sim 30$ mN·m^{-1}; hence, $f \approx 0.4$. From X-ray measurements (J. M. Seddon, G. Cevc, R. D. Kaye, and D. Marsh, unpublished results) $\delta l \approx 0.1$ nm/CH_2; hence, $\delta D \approx 0.033$ nm/CH_2. The corresponding contribution to the transition temperature shift can be estimated from eq 1 and 4:

$$\Delta T_h \approx -[N_A\mu_H/2(R + D)](\delta D/\Delta S_h) \quad (5)$$

Taking $R + D \approx R \approx 2.3$ nm (J. M. Seddon, G. Cevc, R. D. Kaye, and D. Marsh, unpublished results) and $\Delta S_h \approx 17$ J·mol^{-1}·K^{-1} (DHPE) yields $\Delta T_h \approx -13$ °C/CH_2. This is somewhat larger than the measured value of ≈ -8 °C/CH_2 for DHPE, but of the same order of magnitude. Several other factors contribute to the chain length dependence, and the radius R may also change with increasing chain length, but this simple calculation indicates the way in which the geometric effects of increasing chain length tend to stabilize the inverted hexagonal phase.

Salt Dependence. The results of Figures 4 and 5 indicate the way in which high salt concentrations progressively stabilize the inverted hexagonal phase and the lamellar gel phase by decreasing T_h and increasing T_t, respectively. Both effects are consistent with an increasing stabilization of interactions be-

tween the head groups. The mechanism is unlikely to be a simple electrostatic screening of the head-group dipoles, since the salt-induced shifts in T_t for DTPE are much greater than those for DTPC (Figure 8b) despite the similar dipolar character of their head groups. It seems likely that the high concentration of monovalent ions, if not actually displacing water of hydration, certainly affects the interactions of the water molecules with the head-group region. The dielectric constant of bulk water for example is reduced from $\epsilon = 78$ in the absence of salt to $\epsilon = 55$ in 2 M NaCl (Hasted, 1973), which indicates the ability of high salt to decrease the water polarizability. This effective dehydration of the head groups would give rise to the observed shifts, as indicated in Figure 6. For DDPE, the total salt-induced shifts (Figure 4) are $\Delta T_t = +10.5$ °C and $\Delta T_h = -41$ °C. These shifts are similar to those obtained upon lowering the head-group hydration from the limiting values to ~3.5 H_2O/lipid (cf. Figure 6).

Hydration Dependence. The water dependence of the transition temperatures in Figure 6 suggests a different limiting hydration at the gel–fluid transition (~6 H_2O/lipid) than at the hexagonal transition (~9 H_2O/lipid) of DDPE. The difference probably indicates additional water binding with increasing temperature in the fluid L_α phase. Previous estimates of limiting hydration for egg PE are 11 H_2O/lipid by X-ray diffraction at 55 °C in the H_{II} phase (Reiss-Husson, 1967), 7 H_2O/lipid by calorimetry (Ladbrooke & Chapman, 1969), 12 H_2O/lipid by NMR at 22 °C (Finer & Darke, 1974), and 9.2 H_2O/lipid by absorption isotherm at 22 °C (Jendrasiak & Mendible, 1976). For DPPE with 18% water it was found that only 1 H_2O/lipid was bound in the gel phase at the freezing point of the boundary water (Ladbrooke & Chapman, 1969). For dimyristoylphosphatidylserine with a protonated carboxyl group a limiting hydration of 9 H_2O/lipid was estimated, with hydration states of 8 and 7 H_2O/lipid also being observed (Cevc et al., 1981).

The hexagonal and gel-to-fluid transitions shift in opposite directions on decreasing the water content. The most likely explanation is that the lamellar fluid phase binds water more strongly than the lamellar gel phase, whereas the inverted hexagonal phase binds water less strongly than the lamellar L_α phase. A quantitative description of the hydration dependence of the lamellar gel-to-fluid transition has been given by G. Cevc and D. Marsh (unpublished results) in terms of the polarizing field of the lipid polar groups acting on the water molecules. The magnitude of the shift depends both on the change in molecular area and on the change in the polarizing field density at the transition. Both quantities increase at the gel-to-fluid transition, whereas the molecular area of the polar groups decreases at the lamellar–hexagonal transition (Reiss-Husson, 1967; J. M. Seddon, G. Cevc, R. D. Kaye, and D. Marsh, unpublished results), and it is most probable that the polarizing field density also decreases. The result is then that increasing hydration will depress the gel-to-fluid transition and raise the lamellar–hexagonal transition, as observed.

The simple geometric expression in eq 4 also predicts that decreasing water content will favor the inverted hexagonal phase, by inducing a tighter radius of curvature, R. If one neglects changes in D due to changing head group–water interactions the geometric contribution to the transition temperature shift is

$$\Delta T_h \approx [N_A \mu_H / 2(R + D)](D/\Delta S_h)(\delta R/R) \qquad (6)$$

The decrease in radius is given simply by the decrease in the number of water molecules: $\delta R/R \approx (1/2)(1 - d/R)(\delta n_w/n_w)$. Taking $n_w = 9$ H_2O/lipid and $\delta n_w = -1$, this yields an estimate $\Delta T_h \approx -230D$ (nm) °C/H_2O for DDPE. The value for D is likely to be small since the bilayer is the stable low-temperature phase (Israelachvili et al., 1980). A value of $D = 0.04$ nm would yield $\Delta T_h \approx -9$ °C/H_2O which is similar to the experimental value of $\Delta T_h \approx -8$ °C/H_2O.

pH Titration. The total transition temperature shift at the phosphate titration is 7 times greater for the hexagonal transition than for the gel–fluid transition (Figure 7). The ratio of the transition entropies was measured to be approximately ten in 2.4 M NaCl at pH 7, suggesting that this accounts for the greater part of the difference in shift. Similarly the shift at pH 9.3 within the amine titration is 3–4 times greater for the hexagonal transition than for the gel-to-fluid transition. The total titration shift for the latter is −35 °C on fully deprotonating the amine, implying that the full extrapolated shift for the hexagonal transition would be ~+100–140 °C, which is experimentally inaccessible.

Electrostatic effects on the transition temperatures are likely to be relatively small at 2.4 M salt (cf. Cevc et al., 1980). The electrostatic shifts arise from the change in molecular area at the phase transition and would give rise to downward shifts of the gel-to-fluid transition and upward shifts of the hexagonal transition. This is in the direction observed at the amine titration, but in the opposite direction for the phosphate titration. The electrostatic contribution to the total titration shift is given by (Träuble, 1976)

$$\Delta T_t^{GC} = -(2RT/\Delta S_t^*)(c/e)[[(e/ac)^2 + 1]^{1/2} - 1]\Delta a \qquad (7)$$

where $c = (8000\epsilon\epsilon_0 RTc_m)^{1/2}$ and c_m is the molar salt concentration. For area per molecule $a \simeq 0.50$ nm^2, change in a at T_t $\Delta a \simeq 0.11$ nm^2 (J. M. Seddon, G. Cevc, R. D. Kaye, and D. Marsh, unpublished results), and dielectric constant $\epsilon \simeq 50$ (the estimated value over the diffuse double layer), this gives a shift of $\Delta T_t^{GC} = -14$ °C, which is likely to be an overestimate, and thus is unable to account for the major part of the amine titration shift of the gel–fluid transition. The large changes at the amine titration may be attributed mostly to the loss of hydrogen bonding between the $-NH_3^+$ and the PO_4^- groups on deprotonating the $-NH_3^+$ (Eibl & Woolley, 1979; Cevc et al., 1981). The hydrogen bonding tends to stabilize the phase which is less expanded in the head-group region, i.e., the lamellar gel and the inverted hexagonal, giving rise to the observed shifts [see also Boggs et al. (1981)]. Removal of the amine–phosphate hydrogen bond might also result in increased head-group hydration which would also give shifts in the observed direction (cf. Figure 6), but there is currently little evidence for this.

The shifts in both the hexagonal and gel-to-fluid transitions induced by titration of the phosphate group are in the opposite direction to those expected both from electrostatic effects and from loss of NH_3^+–PO_4^- hydrogen bonding on protonating the phosphate. Since the absolute values of the shifts are also considerably smaller than those at the amine titration, it seems likely that the observed shifts are the net effect of opposing mechanisms. The dominant contribution is most probably a dehydration of the phosphate on protonation, which would give rise to an increase in T_t and decrease in T_h as predicted by Figure 6. A similar effect on T_t has been observed for the interaction of protons or sodium ions with phosphatidylserine (Cevc et al., 1981). Eibl & Woolley (1979) have proposed that hydrogen bonding between the partially protonated phosphates gives rise to the increase in T_t of the gel-to-fluid transition. However, this would imply a considerably lower $pK_1^i \simeq 0.5$, which is inconsistent with the analysis of the pK shifts given below.

The apparent pK_i^i of a group at the interface differs from the intrinsic pK_i^w in bulk water because of the shift ΔpK_i^p in

the acid–base equilibrium due to the different surface polarity (Fernández & Fromherz, 1977) and because of the electrostatic enhancement of the surface H^+ concentration which gives rise to a shift ΔpK_i^{el}. For phosphatidylethanolamine bilayers [see, e.g., Cevc et al., (1981)]

$$pK_i^i = pK_i^w \mp |\Delta pK_i^{el}| \pm |\Delta pK_i^{p}| \quad (8)$$

where the upper signs refer to the phosphate titration at pK_1^i and the lower signs to the amine titration at pK_2^i. At $J = 2.4$, ΔpK_1^i $(=pK_1^i - pK_1^w) = +0.48$ and $\Delta pK_2^i = -0.33$; i.e., the values are roughly equal and opposite as predicted by eq 8, with the signs indicating that the polarity shifts dominate, as expected at high salt concentration. At lower ionic strength, $J = 0.1$, the shift $\Delta pK_2^i \simeq +1.1$ has changed sign, and the electrostatic contribution dominates. For an interfacial dielectric constant, $\epsilon \simeq 30$, Fernández & Fromherz (1977) have estimated $|\Delta pK_i^p| = 1.1$. The electrostatic shift predicted by diffuse double layer theory is (Träuble, 1976)

$$\Delta pK_i^{el} = (2/\ln 10) \sinh^{-1} [e/(2ac)] \quad (9)$$

where c is as defined for eq 7. For a molecular area $a \approx 0.5$ nm^2 and $\epsilon \simeq 30$, this gives $|\Delta pK_i^{el}| = 0.98$ for ionic strength $J = 2.4$ and 2.27 for $J = 0.1$. This predicts a total shift $\Delta pK_2^i = -0.12$ at $J = 2.4$ and $\Delta pK_2^i = +1.17$ at $J = 0.1$, in reasonably good agreement with measured values. It should be noted that the electrostatic term may also include a contribution from the amine–phosphate hydrogen bonding, which would give shifts of the same sign.

Head-Group Modification. The effect both of increasing the head-group length (Figure 8a) and of increasing the degree of head-group methylation (Figure 8b) is to produce an approximately linear decrease in the gel-to-fluid transition temperature, T_t. The effects of the head-group length are in contrast with the behavior of the corresponding dipalmitoylphosphatidylcholine analogues for which T_t changes by less than 2 °C over the same range (Bach et al., 1978). This difference suggests that the decrease in transition temperature is not just a result of the increasing bulk of the head group (although this will be relatively greater for phosphatidylethanolamines because of their tighter head-group packing) but may also be due to disruption of hydrogen bonding between the amine and phosphate groups. Head-group methylation will certainly decrease the hydrogen-bonding capabilities of the amine group in addition to increasing head-group bulk. Similar results to those of Figure 8b have also been reported for the gel-to-fluid transition of other phosphatidylethanolamine analogues (Vaughan & Keough, 1974; Gawrisch et al., 1977).

The increase in head-group size (at least initially) shifts the hexagonal transition in the opposite direction to the lamellar gel-to-fluid transition (see Figure 8). The directions of the shifts are also opposite to those obtained on increasing the hydrocarbon chain length (cf. Figure 4), reflecting the inverted nature of the hexagonal phase. This comparison suggests that, although disruption of hydrogen bonding between the head groups will make an important contribution to the transition temperature shifts, the counterbalancing effect of the head-group bulk may also play a role. This geometric contribution can be approximately estimated from eq 5 as was done for the lipid chains. The change in D with increasing head-group volume, v, and thickness, d, is given by $\delta D = -(1/2)(1-f)[\delta d + f(l+d)\delta F_{HD}/F_{HD}]$, where $\delta F_{HD}/F_{HD} \approx \delta v/v$. For DTPE this yields estimates of $\Delta T_h \approx +27$ °C/CH_2 and $\Delta T_h \approx +54$ °C/CH_3 compared with the experimental values of +16 °C/CH_2 and +24 °C/CH_3, respectively. As in the case of the chain length dependence, the estimates are of the same order of magnitude but a factor ~2 times larger than the observed shifts. Possible changes in the radius R with changing head-group structure have again been neglected. However, the results suggest that purely geometric factors do make an appreciable contribution to the stability of the inverted hexagonal phase. The exact results clearly depend on the details of the head-group molecular structure. The delicate balance of opposing molecular forces is also indicated by the appearance of further nonlamellar phases, other than the inverted hexagonal.

Acknowledgments

We thank Fr. B. Hirche for her excellent technical assistance in the synthesis of the lipids.

References

Bach, D., Bursuker, I., Eibl, H., & Miller, I. R. (1978) *Biochim. Biophys. Acta 514*, 310–319.
Boggs, J. M., Stamp, D., Hughes, D. W., & Deber, C. M. (1981) *Biochemistry 20*, 5728–5735.
Cevc, G., Watts, A., & Marsh, D. (1980) *FEBS Lett. 120*, 267–270.
Cevc, G., Watts, A., & Marsh, D. (1981) *Biochemistry 20*, 4955–4965.
Cullis, P. R., & de Kruijff, B. (1979) *Biochim. Biophys. Acta 559*, 399–420.
Eibl, H. (1978) *Proc. Natl. Acad. Sci. U.S.A. 75*, 4074–4077.
Eibl, H., & Nicksch, A. (1978) *Chem. Phys. Lipids 22*, 1–8.
Eibl, H., & Woolley, P. (1979) *Biophys. Chem. 10*, 261–271.
Fernández, M. S., & Fromherz, P. (1977) *J. Phys. Chem. 81*, 1755–1761.
Finer, E. G., & Darke, A. (1974) *Chem. Phys. Lipids 12*, 1–16.
Gawrisch, K., Arnold, K., Rüger, H.-J., Kertscher, P., & Nuhn, P. (1977) *Chem. Phys. Lipids 20*, 285–293.
Harlos, K., & Eibl, H. (1980) *Biochim. Biophys. Acta 601*, 113–122.
Harlos, K., & Eibl, H. (1981) *Biochemistry 20*, 2888–2892.
Hasted, J. B. (1973) *Aqueous Dielectrics*, Chapman and Hall, London.
Israelachvili, J. N., Mitchell, J. D., & Ninham, B. W. (1976) *J. Chem. Soc., Faraday Trans. 2 72*, 1525–1568.
Israelachvili, J. N., Mitchell, J. D., & Ninham, B. W. (1977) *Biochim. Biophys. Acta 470*, 185–201.
Israelachvili, J. N., Marčelja, S., & Horn, R. G. (1980) *Q. Rev. Biophys. 13*, 121–200.
IUPAC (1979) *Ionization Constants of Organic Acids in Solution*, Pergamon Press, Oxford.
Jendrasiak, G. L., & Mendible, J. C. (1976) *Biochim. Biophys. Acta 424*, 149–158.
Ladbrooke, B. D., & Chapman, D. (1969) *Chem. Phys. Lipids 3*, 304–356.
London, E., & Feigenson, G. W. (1979) *J. Lipid Res. 20*, 408–412.
Luzzati, V. (1968) in *Biological Membranes* (Chapman, D., Ed.) Vol. 1, pp 71–123, Academic Press, London.
Marsh, D. (1982) in *Supramolecular Structure and Function* (Pifat, G., & Herak, J., Eds.) Plenum Press, New York.
Marsh, D., & Seddon, J. M. (1982) *Biochim. Biophys. Acta 690*, 117–123.
Nagle, J. F., & Wilkinson, D. A. (1978) *Biophys. J. 23*, 159–175.
Osterberg, R. (1962) *Acta Chem. Scand. 16*, 2434–2451.
Phillips, M. C., Williams, R. M., & Chapman, D. (1969) *Chem. Phys. Lipids 3*, 234–244.

Reiss-Husson, F. (1967) *J. Mol. Biol. 25*, 363–382.
Seddon, J. M. (1980) Ph.D. Thesis, University of London.
Seddon, J. M., Harlos, K., & Marsh, D. (1983) *J. Biol. Chem.* (in press).
Seelig, J. (1981) in *Membranes and Intercellular Communication. Les Houches, 1979* (Balian, R., Charbre, M., & Devaux, P. F., Eds.) pp 36–54, North-Holland, Amsterdam.
Shipley, G. G. (1973) in *Biological Membranes* (Chapman, D., & Wallach, D. F. H., Eds.) Vol. 2, pp 1–89, Academic Press, London.
Stockton, G. W., Polnaszek, C. F., Leitch, L. C., Tulloch, A. P., & Smith, I. C. P. (1974) *Biochem. Biophys. Res. Commun. 60*, 844–850.
Träuble, H. (1976) in *Structure of Biological Membranes* (Abrahamsson, S., & Pascher, I., Eds.) pp 509–550, Plenum Press, New York.
Vaughan, D. J., & Keough, K. M. (1974) *FEBS Lett. 47*, 158–161.
Wilkinson, D. A., & Nagle, J. F. (1981) *Biochemistry 20*, 187–192.

Physical and Chemical Properties of Human Type III Procollagen†

Steve Gerard,‡ Robley C. Williams, Jr., and William M. Mitchell*

ABSTRACT: Type III procollagen was isolated from the serum-free culture media of human foreskin fibroblasts by adsorption to controlled-pore glass beads and chromatography of the eluted procollagen pool on diethylaminoethylcellulose [Gerard, S., & Mitchell, W. M. (1979) *Anal. Biochem. 96*, 433–447]. Sodium dodecyl sulfate ($NaDodSO_4$) electrophoresis in 1% agarose–2% acrylamide gels with or without prior sample reduction revealed the predominance of a band with retarded mobility as compared to human procollagen I [hupro(I)]. Digestion of hupro(III) with pepsin yielded a product whose electrophoretic mobility was retarded for both the intact trimer and its reduced monomeric subunit as compared to that for the respective bands of rat skin (type I) collagen. $NaDodSO_4$–polyacrylamide gel electrophoresis of bacterial collagenase-digested hupro(III) demonstrated disulfide-bonded propeptides which upon reduction were replaced by two distinct monomeric propeptide bands. The amino acid composition of hupro(III) was similar to that of hupro(I) but contained increased amounts of HO–Pro and Cys and less Thr, Ala, Val, and Arg. Sedimentation equilibrium analysis in 1 M $CaCl_2$ yielded at extrapolated zero concentration a M_r of 505 ± 25K. A [hupro(III) – collagen(III)] circular dichroic difference spectrum suggests approximately 10% α helix. The zero-order mutarotation rate of hupro(III) ($v_0 = 55.0 \times 10^{-5}$ s^{-1}) was twice that of hucol(III) ($v_0 = 25.4 \times 10^{-5}$ s^{-1}) at 20 °C, which may reflect the influence of the interchain disulfide-bonded carboxyl propeptides on the process of collagen fold formation.

Type III collagen has been referred to as the fetal collagen, since it is relatively most predominant in the skin during fetal life (Epstein, 1974). However, this genetic type is also predominant in the arterial wall, intestine, and muscle and generally codistributes elsewhere in diminished relative proportion with type I collagen, excluding bone and tendon [for reviews, see Eyre (1980), Bornstein & Traub (1979), and Prockop et al. (1979)]. Type I and type III collagen, which together represent the majority of the body's interstitial collagen, are chemically similar, but type III is distinguished by about one-third more hydroxyproline and the presence of interchain disulfide bonds at the carboxyl terminus of the triple helical sequences (Chung et al., 1974; Glanville et al., 1976). Fibrils prepared in vitro from type I and type III collagens (Wiedemann et al., 1975) display a similar periodicity, although the cross-sectional diameter of type I appears to be greater than that of type III. This is consistent with the identification of type III collagen as one of the macromolecular constituents of the thin reticulin fibers which are seen in liver and spleen (Nowack et al., 1976a).

Procollagen represents the soluble biosynthetic precursor to the collagen molecule. Though most of the studies to date detailing procollagen structure have come from nonhuman systems, it appears that types I and III procollagen are very similar, both containing trimeric propeptides at each end which include a short collagen sequence in the amino terminus [for a review, see Timpl & Glanville (1981)] and an interchain disulfide-bonded structure at the carboxyl end [for reviews, see Eyre (1980), Bornstein & Traub (1979), Prockop et al. (1979)]. Type III procollagen, but not type I, however, contains additional interchain disulfide bonds between the amino propeptides (Bruckner et al., 1978; Fessler & Fessler, 1979; Nowack et al., 1976b; Uitto et al., 1980).

During intracellular procollagen biosynthesis, three separate precursor chains presumably associate in proper alignment such that subsequent formation of the triple helix ensues [for reviews, see Fessler & Fessler (1978) and Prockop et al. (1979)]. Since helical folding in vitro of free collagen chains in solution proceeds very slowly and incompletely (Altgelt et al., 1961), it was postulated by Speakman (1971) that the precursor sequences might function as "registration peptides" to facilitate the initial alignment of the three separate polypeptide chains and, thereby, subsequent formation of the triple helix. Although it was originally suggested that these registration peptides were located in the amino end of the proα[1]

† From the Departments of Pathology (S.G. and W.M.M.) and Molecular Biology (R.C.W.), Vanderbilt University, Nashville, Tennessee 37232. *Received May 3, 1982; revised manuscript received November 1, 1982.* Supported in part by U.S. Public Health Service Grants AM-18222 and GM 25638.

‡ Present address: Department of Laboratory Medicine, University of California, San Francisco, San Francisco, CA 94143.

[1] Abbreviations: DEAE, diethylaminoethyl; Tris, tris(hydroxymethyl)aminomethane; EDTA, ethylenediaminetetraacetic acid; CD, circular dichroism; $NaDodSO_4$, sodium dodecyl sulfate; hupro(III), human type III procollagen; hucol(III), human type III collagen; proα, collagen precursor chain containing amino and carboxyl propeptides [since only one type of chain has been identified to date for type III collagen, we have dropped the "1" designation in reference to proα(III) or α(III) chains]; proγ, three proα chains interchain linked by disulfide bonds; pγ, proteolytically altered proγ chains missing propeptides on one end; pN-collagen, pγ containing amino but not carboxyl propeptides.

0006-2960/83/0422-1289$01.50/0